Title

The effects of surrounding buildings on wind pressure distributions and natural ventilation in long building rows

Authors

Bauman, Fred
Ernest, D.
Arens, Edward A

Publication Date

1988

Peer reviewed

OT-88-13-3

THE EFFECTS OF SURROUNDING BUILDINGS ON WIND PRESSURE DISTRIBUTIONS AND NATURAL VENTILATION IN LONG BUILDING ROWS

F.S. Bauman, P.E. *ASHRAE Member*
D.R. Ernest
E.A. Arens, Ph.D. *ASHRAE Member*

ABSTRACT

To predict the performance of a naturally ventilated building, estimates of the wind-induced surface pressure distribution are needed. In urban environments, where buildings are grouped closely together, these surface pressures will be strongly influenced by the surrounding structures. In addition, the sheltering effect of the surrounding built-up environment can make it more difficult to obtain large enough pressure differences across a building necessary to produce adequate natural ventilation airflow rates. This paper describes the results of a wind tunnel investigation of wind pressure distributions over an attached two-story shop or housing unit contained in long building rows of the variety that are commonly found in densely populated commercial centers of Southeast Asia (shophouse) and other urban settings (British row house). Surface pressure measurements were made on a 1:125 scale model as a function of wind direction, spacing between adjacent building rows, and building geometry. Simplified correlations are developed to predict the measured surface pressure coefficients. The jack roof, a roof-level ventilation device, is a key architectural feature of the test model. Using the developed correlations, the characteristics of the ventilation performance of the jack roof are discussed and compared to those for other flow configurations. The jack roof demonstrates significant potential to be an effective natural ventilation design for densely built-up urban areas.

INTRODUCTION

Buildings in hot and humid climates have been traditionally cooled by ventilation. Ventilative air movement in the building interior acts to cool the occupants in two ways. First, it cools the occupant directly by increasing the convective and evaporative heat transfer from the body surface. Second, it cools the occupant indirectly by removing heat stored in the building structure. Traditional buildings are operated in either or both modes depending on the climate. Internal airflows in such naturally ventilated buildings can be (1) wind-driven, resulting from the external wind pressure field, and (2) buoyancy-driven, resulting from the temperature differences between the building interior and exterior. Even in relatively light winds and under typical interior-exterior temperature differences, wind pressure forces, rather than buoyancy forces, are the dominant cause of naturally driven ventilation.

In urban environments, where buildings are grouped closely together, the wind-induced surface pressure distribution on a building, as well as the local wind velocity field around a given building, will be strongly influenced by the surrounding structures. In addition, the sheltering effect of the surrounding built-up environment can make it more difficult to obtain large enough pressure differences across a building necessary to produce adequate ventilation airflow rates.

Previous related studies have looked at the effect of vegetation windbreaks and fences on wind pressures and the resulting air infiltration energy losses/gains in residential housing. The studies were done at small scale in a wind tunnel (Mattingly and Peters 1977) and at full scale in the field (Mattingly et al. 1979). Peterka and Cermak (1975) performed a wind tunnel study of wind velocities in the wakes of freestanding buildings. The effect of a single adjacent upwind building on wind pressures on a rectangular building was the subject of a wind tunnel study by Peterka et al. (1979). Aynsley (1979) described the influence of a single upwind row of houses on the mean windward and leeward surface pressures of a house for a limited number of wind directions and building spacings. A thorough review of recent wind tunnel studies of wind loads on low rise buildings was reported by Holmes (1983).

Fred Bauman, Associate Development Engineer, David Ernest, Ph.D. candidate, and Edward Arens, Professor, Building Science Laboratory, Department of Architecture, University of California, Berkeley, CA 94720.

The effect of a group of surrounding buildings has been studied in a series of wind tunnel experiments performed in the United Kingdom. Soliman (1973) studied a cuboid and Lee et al. (1979) studied a rectangular model at several geometric aspect ratios. In both studies, the test model was surrounded by various arrays of identically shaped models. The results of Lee et al. give reductions in surface pressures on the test model as a function of building alongwind spacing, the layout of the buildings in the crosswind direction (two grid patterns were examined), and the wind approach direction over either layout. The results of the study show wind pressure reductions of up to 90% resulting from wind blockage by upwind buildings. However, there is a variability of 80% depending on the configuration of the buildings. Hussain and Lee (1980) present additional wind tunnel results on the surface pressure fields and airflow regimes between buildings for rectangular blocks representative of low-rise buildings in suburban areas.

Wiren (1985) has performed an extensive wind tunnel study of the wind pressure effects on a 1 1/2-story single-family house surrounded by identical models in various regular arrays. Measurements were made for an isolated model, model with one upwind model, model with two adjacent models, and model within a large group of models. Unlike the previous flat-roofed models, the models used in Wiren's study had a roof pitch angle of 45 degrees. His tests indicated that the maximum reduction in ventilation airflow rate, obtained with three rows of houses surrounding the test house, was about 40%. The above wind tunnel study was recently repeated for two-story terrace houses (Wiren 1987).

Given a set of pressure distribution data for a building, simplified calculation techniques exist for estimating the amount of infiltration airflow through cracks or other small leakage areas or ventilation airflow through larger wall openings. The internal airflow is driven by the pressure difference between surfaces containing flow inlets and outlets. Ventilation airflow equations have been described by Aynsley (1982) for a series of openings without internal flow branching and by Vickery (1981) for multiple openings with significant internal flow branching. The models make use of discharge coefficients derived from ventilation duct studies, obviously an approximation for typical building ventilation openings. As with the current wind tunnel study, the vast majority of available surface pressure data have been collected for solid models. The presence of flow inlets and outlets will influence the surface pressure in the vicinity of the opening. However, investigations by Vickery et al. (1983) have shown that the effect of small openings (less than 20% of total wall area) on solid-building pressure data does not significantly affect the accuracy of the above flow models, if the openings are in walls. Vickery did find that the model predictions (based on solid-building pressure data) significantly overpredicted the measured internal airflow for small roof-level outlets. More work is needed to fully understand the performance of roof-level ventilation openings.

Although the wind pressure will vary over a given building surface, particularly near the edges, for low-rise buildings these variations will not have a significant effect on ventilation airflow predictions. As a result, a single average pressure over an entire building surface is typically used in the above airflow models. Swami and Chandra (1987) found that the error produced by using average vs. local pressure data was about 5%. Similarly, Wiren (1985) indicated an error of less than 10%.

Correlations of the type reported in the current study, along with the appropriate airflow models, can be usefully incorporated into ventilation design manuals using manual methods or small computer calculation techniques. Manual design procedures for natural ventilation have been reported by Chandra (1983), Arens and Watanabe (1986), and Swami and Chandra (1987). Pressure coefficient correlations can also be added to large hourly simulation programs (e.g., ESP) containing more sophisticated internal airflow calculation subroutines (Clarke 1986).

PRESENT INVESTIGATION

The building to be studied is a narrow attached shophouse, commonly found in the densely populated commercial centers of Southeast Asian towns and cities, as well as other urban settings (e.g., the British row house). Figure 1A shows a perspective cut-away drawing of the shophouse model, which consists of two identical two-story units separated by a central walled courtyard. In the figure, the facing building and courtyard walls are removed. Each unit has a gable roof with a small raised roof vent structure (jack roof) at the roof peak. Shophouses are contained in long rows of identical units, each separated from its adjoining units by roof parapets (Figure 1B).

As described above, previous wind tunnel experiments on the influence of surrounding obstructions have largely focused on three-dimensional models (typically cubical in shape) surrounded by elements of identical size and shape in some sort of grid pattern. The present study will address a configuration in which the test building unit is located near the middle of a long building row, surrounded by other parallel building rows of identical size and shape. In this arrangement, wind effects in the immediate vicinity of the test model will be largely independent of the ends of the building rows. In other words, the position of the unit within the building row will not be a significant parameter, which is expected to be the case for a large majority of such shophouses.

A key architectural feature of the shophouse design is the jack roof, designed to promote ventilation airflow through the building. The positioning of the jack roof at the roof peak is crucial to its ventilation performance, particularly in built-up urban environments where surrounding buildings can have significant shielding effects. Proposed correction factors based on generalized shielding indicate that the ventilation airflow rates can be reduced by a factor of two to three in typical urban settings, compared to those for the same building in exposed, rural terrain (Sherman and Grimsrud 1982).

As shown in the schematic flow diagrams of Figure 2, the jack roof can be operated in several different modes. With both sides of the jack roof open, wind-driven airflow through the jack roof will induce air to be extracted from the building (Figure 2A). The performance of roof ventilators using this principle has been studied by Wannenburg (1957). If wind entering the windward side of the jack roof is diverted down into the building (Figure 2B), its ventilation principle will resemble that of wind towers commonly found in Middle Eastern architecture (Bookhash 1981). If only the leeward side of the jack roof is allowed to be open, the strong negative pressures will promote the suction of air out through this surface (Figure 2C). One jack roof design of this type has been described by Fairey and Bettencourt (1981). A model of a full-scale laboratory building incorporating a jack roof has been the subject of a wind tunnel investigation by Cermak et al. (1981). Vickery et al. (1983) performed wind tunnel experiments to compare the measured ventilation airflow rates through a ridge vent (located on the leeward side of a standard gable roof) with those predicted by a simplified model for cross-flow ventilation. When little or no winds are present, all jack roof configurations are effective at promoting stack-driven ventilation (Figure 2D).

The objectives of the current study are to:

1. Determine average wind pressures on the external surfaces of a shophouse located in a typical urban environment;
2. Develop simplified correlations to predict the average surface pressure coefficients as a function of building spacing, wind direction, and building geometry; and
3. Study the potential ventilation performance of the jack roof design.

EXPERIMENTAL METHODS

Boundary Layer Simulation

The study was conducted in an open circuit, boundary layer wind tunnel (BLWT) located in a university laboratory (see Figure 3). The building configuration under investigation in the current experiments can be characterized as a low urban environment with long rows of relatively closely spaced two- to three-story buildings extending for large distances in any direction. The approaching boundary layer flow was simulated in the wind tunnel using techniques similar to those described by Cook (1982).

Velocity and turbulence intensity profiles were measured in the wind tunnel at the front edge of the turntable to document the approach wind conditions. These measured profiles are presented in Figures 4A and 4B. The velocity data were used to produce a regression fit with the logarithmic velocity profile for a thermally neutral atmosphere given below:

$$U(z) = (u*/k) \ln[(z-d)/z_0] \quad (1)$$

where

$U(z)$	= mean velocity at height z (m/s)
$u*$	= friction velocity (m/s)
k	= von Karman's constant (0.4)
z_0	= roughness length (m)
d	= displacement height (m)

The regression fit in Figure 4A produced a roughness length (z_0) of 0.19 in (4.8 mm) (full-scale z_0 = 2.0 ft [0.6 m]) for a displacement height (d) of 2.0 in (50 mm) (full-scale d = 20.5 ft [6.25 m]), well within the accepted range of values prescribed by Engineering Sciences Data Unit (1982; 1974, 1975, 1985) for low urban terrain. In Figure 4B the measured turbulence intensities correspond well to values recommended by ESDU (1984) for the lower region of the atmospheric boundary layer. The power spectrum was measured at a height of 5.9 in (150 mm) and matched to that recommended by ESDU (1974, 1975, 1985). Using the method described by Cook (1978), the simulated turbulence scale, and therefore the most appropriate model scale, was calculated to be 1:130, an excellent match with the model scale used.

Building Models

A model containing two identical building units was fabricated out of 1/8 in (3 mm) acrylic sheet at a scale of 1:125, based on the typical shophouse configuration shown in Figure 1A. The two model units were connected by a central courtyard area and, together, represent a single attached shophouse unit located within a long double row of similar building units. Each double row is separated from adjacent identical double rows by a space representative of a street or alley (Figure 1B). The key architectural features of the shophouse model are as follows:

-- The overall dimensions of each model unit are H = 3.1 in (80 mm), L = 3.1 in (80 mm), and W = 1.6 in (40 mm), representative of a two-story shophouse, 33 ft (10 m) high to the top of the jack roof, 33 ft (10 m) long, and 16.5 ft (5 m) wide.
-- The roof pitch angle (α) is fixed at 20 degrees.
-- A 0.24 in (6 mm) high jack roof (2.5 ft [0.75 m] full scale) is located at the roof peak and covers the top third of the roof.
-- Parapets, equal in height to the jack roof, extend along both sides of the pitched roof, separating each adjacent shophouse unit.
-- Both the jack roof and parapets are removable, allowing alternate roof configurations to be investigated.
-- Each central courtyard is separated from adjacent courtyards by walls of variable height.

The surrounding building models were all constructed from extruded polystyrene foam board. The 1:125 scale model produced a maximum wind tunnel blockage of 4.9%. No corrections were made to the pressure measurements obtained with this configuration.

When the height of the surrounding environment (adjacent structures, trees, etc.) is on the same order as the height of the subject building, as in the current study, then the surrounding buildings must also be modeled in detail. For low-rise suburban terrain, the extent of this modeling is recommended to be a radius of ten building heights (Aynsley 1985). In the current model setup, surrounding buildings were modeled to the edge of the turntable, having a radius of 3.3 ft (1 m). Further upwind of the turntable, general roughness elements on the wind tunnel floor were used to simulate the characteristics of the approaching boundary layer flow.

None of the ventilation inlets and outlets (e.g., windows or jack roof openings) was included in the models. Rather, pressure taps were installed at the appropriate locations on the solid model surfaces. Figures 5A and 5B are exploded plan views of the two models showing the pressure measurement (tap) locations for the standard roof and the jack roof designs. During all tests the models were configured such that Model #1 was the upwind model and Model #2 was the downwind model. For each model unit 18 taps were monitored for the standard gable roof model, and for the jack roof design, an additional 4 taps for a total of 22 taps were monitored. Tap locations were selected to allow the measured pressures to represent averages over areas of equal size on a given model surface.

Pressure Measurements

Pressure measurements were made with two differential pressure transducers. One transducer monitored the pressure taps on the model surfaces. The taps were connected via equal lengths of 0.063 in (1.6 mm) O.D. vinyl tubing to a pressure switch that allowed up to 48 pressure lines to be connected to a single transducer. The second transducer monitored the dynamic pressure at the reference location. A pitot tube suspended from the ceiling (see Figure 3) was used to measure the reference conditions. With a mean reference velocity at the pitot tube of 1710 fpm (8.7 m/s), each pressure measurement consisted of simultaneous readings from the two pressure transducers. The transducers were sampled at a rate of 30 readings per second for a duration of 30 seconds. Upon switching to a new port location of the fluid switch wafer, a delay of 15 seconds was implemented to allow the line pressure to stabilize at its new mean value.

In the current study the pressure coefficients were normalized by the dynamic pressure at the equivalent 33-foot (10-meter) height, the most common weather station height. This allows the results to be related to full-scale conditions. Since simultaneous measurements at the 10-meter full-scale reference height (80 mm at wind tunnel scale) could not be made without disturbing the model measurements, the pressure coefficient was determined in two stages as defined below:

$$\begin{aligned} C_p &= (P-P_s)/(0.5\rho U_{10}^2) \\ &= (P-P_s)/P_d * P_d/(0.5\rho U_{10}^2) \\ &= C_{p,ref} * D \end{aligned} \qquad (2)$$

where

C_p = mean pressure coefficient normalized by dynamic pressure at equivalent 10-meter height
$C_{p,ref}$ = mean pressure coefficient normalized by dynamic pressure at stationary reference pitot tube
P = mean pressure at building surface (Pa)
P_s = mean static reference pressure (Pa)
P_d = mean dynamic reference pressure = P_t-P_s (Pa)
P_t = mean total reference pressure (Pa)
ρ = density of air (kg/m^3)
D = dynamic pressure height correction factor (9.47)
U_{10} = mean velocity at equivalent 10-meter height (m/s)

In Equation 2, $C_{p,ref}$ was measured directly as described above. The dynamic pressure height correction factor, D, was determined from a separate measurement with a hot-film anemometer placed at the equivalent 10-meter height (3.1 in [80 mm]). The static pressure was assumed to be constant at both the reference and 3.1 in heights, and no static pressure correction factor was applied in the equation. All mean surface pressure coefficients presented in this report are of the form defined by Equation 2.

Full details of the experimental methods are described in Bauman et al. (1988).

PROGRAM OF STUDY

Building surface pressures were measured in response to a number of parameters varied over the ranges defined below. Refer to Figures 6A, 6B, and 6C for illustrations of the typical model layout, roof configurations, and courtyard configurations.

1) wind direction (θ):	0°, 15°, 30°, 45°, 60°, 75°, 90° from normal
2) spacing between double rows (s):	$S = s/H = 0.5, 1, 2, 3, 4, 5$
3) courtyard spacing (s_c):	$S_c = s_c/H = 0.25, 0.5, 1$
4) courtyard wall height (h_c):	$H_c = h_c/H_e = 0, 0.5, 1$
5) roof configuration	a) without jack roof, without parapet (NJ,NP) b) with jack roof, without parapet (J,NP) c) with jack roof, with parapet (J,P)

where

H = building height
H_e = eave height (maximum courtyard height)

For each of the above three roof configurations, seven wind directions and six row spacings were investigated for a total of 42 measured pressure distributions. During each series of tests, the courtyard was held at a fixed configuration. For the standard gable roof (without jack roof, without parapet), this was $S_c = 0.5$ and $H_c = 0$. For the two jack roof configurations, this was $S_c = 1$, $H_c = 1$. Variations in the courtyard spacing and geometry were studied only for a fixed upwind row spacing of $S = 1$ and for the jack roof with parapet roof configuration. These procedural simplifications were justified (1) due to the observed insensitivity of courtyard surface pressures to variations in row spacing (S), (2) due to the relatively small effect of roof configuration on courtyard surface pressures, (3) due to the very repeatable dependence of courtyard surface pressures on wind direction, and (4) in the interest of reducing the number of wind tunnel tests to a manageable number.

In the current study, for each of the major ventilation surfaces (i.e., surfaces where ventilation inlets and outlets would typically be located), a single surface averaged pressure measurement is reported. Due to the largely two-dimensional geometry of the long building models, pressures showed little variation laterally across the front and back facades of the models. For these surfaces, a representative average pressure could be obtained from the two centrally located taps. In addition, localized pressure coefficients on both vertical surfaces facing the central courtyard were found to be very similar in magnitude for all model configurations tested. For this reason a single average courtyard pressure coefficient is reported. The individual taps used to produce the average pressure for each surface are identified in Table 1.

RESULTS AND DISCUSSION

Correlation Development

The pressure measurement results have been analyzed using a PC-based data analysis and graphics program. Using a step-wise multiple linear regression fitting routine, simplified correlations have been developed, as a function of wind direction and row spacing, which predict the average pressure coefficients for many of the surfaces with a high degree of accuracy. All correlation equations took the same general form that is given below:

$$C_p = C_0 + \sum_{i=1}^{N} C_i.F_i \qquad (3)$$

where

C_i ($i = 0,1,...,N$) are constants defined in Tables 2 and 3
F_i ($i = 1,2,...,N$) are functions defined in Tables 2 and 3

Table 2A presents the correlations for the standard gable roof building (NJ,NP); Table 2B presents the results for the two jack roof buildings ((J,NP) and (J,P)); and Table 3 presents the results for the variable courtyard configuration. It was found that for most building surfaces, the pressure coefficients could be correlated with only three or fewer terms in the above equation (all significance levels were $< 10^{-4}$). One term (C_0) was a constant. The "$\cos^2\theta$" term was used to account for wind angle dependence. The "$\cos\theta * S$" and "$\cos\theta * \ln(S)$" terms account for the decreasing effect of spacing at larger wind angles, when the wind is channeled down the streets. The "$\cos^2(\theta-\pi/4)$" term reflects the observed peak pressures on the front jack roof near a wind angle of 45°. The "$H_c * S_c$" term in Table 3 accounts for the increased sensitivity to courtyard wall height with increasing courtyard spacing. In the correlation tables and following figures, the model configurations are identified according to the key shown in Table 4.

Pressure Distribution on Model #1

Figures 7A and 7B illustrate the characteristics of the pressure distribution over Model #1 (upwind model) for one model configuration: jack roof with parapet and upwind spacing of S = 2. Figure 7A shows mean pressure coefficients as a function of tap location for the front of Model #1, and Figure 7B shows the results for the back of the model. The results are shown for three wind directions (0°, 45°, and 90°). Note that the lines on both figures do not represent measured data but are shown only to illustrate the trends in the results. The observations are as follows:

1. Pressures on the windward side of the model exhibit large differences between individual surfaces. This is due to the strong incident winds on some of the surfaces, along with flow separation at several locations (front edge of lower roof, top of jack roof, and, for wind angles of 45° and 90°, top of parapets).
2. In contrast, the pressures on the leeward side of the model are nearly constant at all tap locations, for a given wind angle. This clearly demonstrates how the wake region encompasses the entire leeward side of the model.
3. At 90° wind angle, the pressure coefficients for both sides of the model are very nearly equal and approach zero. This is an expected result as the wind is channeled between building rows on both sides of the model.
4. The largest pressures on the windward side of the model are obtained for a wind direction of 45° on the lower front roof (taps #8 and #9), and on half of the front jack roof (tap #12). In both cases, the presence of the parapets strongly influences the pressures at these locations. These roof pressures will be influenced by changes in the roof slope ($\alpha = 20°$ in current study).
5. The largest negative pressures on the leeward side of the model occur on the jack roof, due to its close proximity to the strong separation from the roof peak.
6. For the 0° wind angle, all pressure coefficients on the windward side of the model are negative or zero. This indicates that even at an upwind row spacing of S = 2, the front of the model lies in the wake region of the upwind model.

Measurement and Correlation Results

Figures 8A and 8B present two examples of measured data and their comparison to the correlation predictions of Table 2. Figure 8A presents results for the front facade of Model #1 with the jack roof but without parapets (J,NP). The observations are as follows:

1. The results follow similar trends for all three roof designs.
2. Pressure increases with increasing spacing. At small spacings and small wind angles, the front facade falls in the wake region of the upwind building row, as indicated by the large negative pressure coefficients.
3. As expected, as the wind direction approaches 90°, the wind is channeled down the streets between the building rows, resulting in similar surface pressure coefficients for all three model configurations. The results approach

zero at 90° for all spacings.
4. For the two models with the jack roof, the existence of the parapet had very little effect, as a single correlation in Table 2B was used to fit both sets of data.
5. The model with the standard gable roof (NJ,NP) showed slightly higher pressures compared to the two jack roof models. This was particularly evident at small wind angles, where the shielding effect of the taller upwind building row (with the jack roof) was strongest.
6. Excellent agreement ($R^2 = 0.95$) was obtained between the measured data and correlation predictions.

Figure 8B presents the measured results and the correlation predictions for the front jack roof for Model #1 (J,NP). The observations are as follows:

1. The results are much less sensitive to upwind spacing than the front facade, as the jack roof is more consistently exposed to the ambient winds.
2. At 0° wind angle, the pressure coefficents are either negative or close to zero, demonstrating the sheltering effect of the upwind building row.
3. The figure indicates that for spacings in the range of 2 to 3, the measured pressures are approaching their maximum values at a wind angle of around 45°. Increasing the upwind spacing any further does not produce a significant increase in pressure on this surface. If a design objective is to maximize pressure on the front of the jack roof (presumably to increase the induced volume of airflow from the building interior out the back of the jack roof [see Figure 2A]), a spacing of S = 2 to 3 may be close to an optimum choice in urban areas where large spaces between buildings are not an option.
4. A comparison of the data in Figure 8B with results for the front jack roof from the model having parapets (J,P) found the surprising result that, although local pressures were strongly influenced, the surface-averaged pressure coefficients were quite similar in magnitude. A single correlation for the front jack roof (with and without parapets) is reported in Table 2B.
5. The influence of the more complex geometry of the jack roof made it more difficult to achieve as accurate of a correlation fit ($R^2 = 0.84$), although reasonable agreement was obtained between a single correlation and the results of both jack roof model tests (with and without parapets).

Measurement results for the other three surfaces (back jack roof, back facade, and courtyard) are not presented here, but the correlation equations in Table 2 indicate similar trends for all of them. Since these surfaces were within the wake region of the immediate upwind building, all experienced large negative pressures at normal wind incidence, making them good choices as ventilation outlets. Pressure coefficients increased with increasing wind angle, approaching zero at 90°. Pressures were found to be virtually independent of upwind row spacing (S) for both the back jack roof and back facade, as excellent correlation fits (dependent only on wind direction) were obtained. Courtyard pressures were only very weakly dependent on spacing.

Table 3 presents the correlation equation for the courtyard pressure coefficient in response to variations in courtyard wall height (H_c) and courtyard spacing (S_c). The results were obtained for an upwind row spacing of S = 1 and were found to be only weakly dependent on the courtyard geometry. A full-height courtyard wall ($H_c = 1$) does provide some amount of protection in the courtyard, slightly reducing the pressure coefficients for all wind directions, especially for larger-sized courtyards.

All measurement results and further discussions are contained in Bauman et al. (1988).

Use of Correlation Tables

The correlation equations contained in Tables 2 and 3 can be used to predict average pressure coefficients on similar full-scale long building rows. The predictions are applicable to building units located away from the influence of the ends of the building rows. For all surfaces except the courtyard, average pressure coefficients can be calculated directly from Table 2 for the given building configuration. For small row spacings, $0.25 \leq S \leq 1$, use the appropriate correlation with S = 1.

Example 1: Find the average pressure coefficient for the front facade of a building with a jack roof (with or without parapets) for a wind angle of 45° and an upwind row spacing of 2.

From Table 2B:

$$C_p = 0.062 - 0.945(\cos 45°)^2 + 0.237(\cos 45°)(2)$$

$$C_p = -0.075$$

The combined effects of courtyard configuration (S_c, H_c) and upwind spacing (S) can be computed using both Tables 2 and 3 as explained below. In performing this calculation, it is assumed that these effects are additive. (1) Use Table 3 to determine the value of C_p for the given values of S_c and H_c. (2) Add the additional contribution due to the effect of upwind row spacing (S) from Table 2. This corresponds to only the one term in Table 2 dependent on S and only for the contribution for S > 1, the value of S for which Table 3 was derived. (3) Add the results from steps 1 and 2.

Example 2: Find the average courtyard pressure coefficient for the following configuration:
$\theta = 25°$, $S = 2.5$, $H_c = 0.5$, $S_c = 0.75$.

(1) From Table 3:

$$C_p(3) = -0.471(\cos 25°)^2 - 0.147(0.5)(0.75)$$

$$C_p(3) = -0.442$$

(2) From Table 2 (spacing contribution only):

$$C_p(2) = -0.057(\cos 25°)(2.5 - 1)$$

$$C_p(2) = -0.077$$

(3) Total pressure coefficient:

$$C_p = C_p(3) + C_p(2) = -0.52$$

Wind Pressure Differences: Ventilation Potential

Given a set of pressure distribution data for a building, simplified models can be used to estimate the amount of cross-ventilation airflow through inlets and outlets located on the building walls. The equation for calculating the air-flow through a cross-ventilated building with one effective inlet and one effective outlet is given below (Swami and Chandra 1987).

$$Q = C_d A_e U_{ref} (\Delta C_p)^{1/2} \quad (4)$$

where

Q = airflow (m^3/s)
C_d = discharge coefficient
A_e = effective area of inlet and outlet (m^2)
ΔC_p = pressure coefficient difference across the inlet and outlet

Using Equation 4 as a guide, the relative ventilation effectiveness of various combinations of surfaces has been compared by calculating the square root of the mean pressure coefficient differences between the selected surfaces. Although the specific values of the discharge coefficient, inlet and outlet areas, and reference velocity will directly influence the obtained airflow volume, an analysis of $(\Delta C_p)^{1/2}$ helps to clarify the characteristic performance of the ventilation configuration. In the following series of figures, the quantity $(\Delta C_p)/|\Delta C_p|^{1/2}$, based on the developed correlation predictions, is plotted for selected pairs of surfaces on the front and back jack roof and front and back facades of Model #1. By using this quantity, negative values represent a reversal of the flow direction through the building. Note that the back facade of Model #1 is part of the courtyard.

Figure 9 presents the pressure difference coefficients between the front and back facades of the model with the standard gable roof (NJ,NP). Without a ventilation opening on the roof, this is the most appropriate wind pressure difference to drive cross-ventilation of the building. As expected, the pressure difference increases with increasing spacing. At upwind spacings of $S \leq 1$, the ventilation potential is negligible due to the strong sheltering effect of the adjacent buildings.

Since the back of the jack roof tends to have the largest negative pressures for all leeward building surfaces, using this surface as the ventilation outlet will improve the potential ventilation airflow (see Figure 2C). Figure 10A shows pressure difference results between the front facade and back of the jack roof. The pressure differences are quite comparable to the previous results for front to back facade (Figure 9), although larger values are obtained at the smallest spacing (S=1). Figure 10B shows pressure difference results between the back facade and the back of the jack roof. The lower pressure differences are indicative of the fairly uniform pressure distribution over all leeward surfaces of the building, although some ventilation potential does exist.

In the above flow configurations as well as others incorporating the jack roof, it must be kept in mind that the accuracy of Equation 4 for roof-level openings may be unreliable (Vickery et al.1983). In addition, the smaller size of the jack roof compared to typical windows in the building walls could reduce the effective inlet/outlet areas. However, in the example discussed above (Figures 10A and 10B), both the front and back facades of the building can act as flow inlets.

If the front of the jack roof is used as a ventilation flow inlet (Figures 2A and 2B), generally higher pressure differences will be produced at small row spacings, as this surface experiences higher pressures than the more sheltered front facade of the building. Figure 11A presents the pressure difference results between the front jack roof and the back facade, and Figure 11B presents results between the front jack roof and the front facade. In both figures, it is seen that higher pressure differences exist at small spacings compared to the previous flow configurations discussed above. In fact, the pressure differences between the front jack roof and the front facade attain their maximum values at the smallest row spacings, when the front facade is heavily sheltered (Figure 11B). For the jack roof to be used effectively as a flow inlet, the roof slope must be large enough (20° in the present study) to produce positive pressure differences between the front (windward) jack roof surface and the surface(s) containing ventilation outlets.

Figure 12 shows the pressure differences between the front and back of the jack roof. A strong airflow directly through the jack roof could be used to promote ventilation of the building by entraining air from the spaces below the jack roof (Figure 2A). If air is diverted down into the building, the ventilation principle would resemble that of a wind tower (Figure 2B). The cross-ventilation flow model (Equation 3) would clearly have limitations if applied to either of these two flow configurations. Nevertheless, an important performance characteristic of the jack roof design can be identified, as the results of Figure 12 are very insensitive to building spacing. This has important implications for use of the jack roof design in urban environments where buildings are often located quite close to each other. If an adequate ventilation airflow can be achieved for this configuration, the jack roof may be quite consistent in its ability to provide ventilation over a wide range of building spacings.

CONCLUSIONS

Wind tunnel measurements have been made of the wind pressure distributions over an attached two-story shop or housing unit contained in long building rows for a range of wind directions, building spacings, and building geometries. Simplified correlations have been developed, which quite accurately predict the average pressure coefficients for the configurations tested. The results have been analyzed to assess the nature of wind pressure effects caused by surrounding building rows of the same size. The jack roof along with the choice of inlet and outlet locations have been discussed in an effort to identify promising naturally ventilated designs in closely spaced buildings typical of urban environments. The major conclusions are as follows:

1. The jack roof has the potential to be an effective ventilation design for urban settings.
2. Compared to standard cross-ventilation designs, the jack roof demonstrates improved ventilation potential at the small building spacings typically found in urban areas.
3. At small building spacings ($S \leq 1$), cross-ventilation designs showed no potential for providing airflow through the building.
4. Since the jack roof element is located at the top of the building, for the building configurations tested it is more consistently exposed to stronger wind conditions. As a result, the performance of the jack roof is less dependent on variations in building spacing.
5. Strong negative pressures were consistently obtained on the back of the jack roof, making it a good choice for a ventilation flow outlet.
6. The results indicate that to achieve optimal performance of a ventilation design incorporating a jack roof, different operating modes may be necessary. In other words, the best choices of flow inlets and outlets may be dependent on building spacing and wind direction.
7. The entire courtyard area was found to consistently fall within the wake flow region of the upwind building row. This was because the largest courtyard spacing tested was $S_c = 1$.
8. Pressure coefficients on all leeward surfaces and the courtyard were found to be practically independent of upwind row spacing and dependent only on wind direction.

Future related work is needed to address the following important areas:

1. Development of algorithms to predict internal ventilation airflow for configurations using roof-level inlets and outlets.
2. Investigations of the effect of internal partitions and obstructions on internal airflows, and incorporation of these results into airflow prediction algorithms.
3. Measurement of building surface pressure distributions for other important building configurations for natural ventilation design.
4. Determination of microclimatic effects on ambient wind conditions.
5. Development of design methods, tools, and guidelines for natural ventilation design.

REFERENCES

Arens, E.A., and Watanabe, N. 1986. "A method for designing naturally cooled buildings using bin climate data." ASHRAE Transactions, Vol. 92, Pt. 2.

Aynsley, R.M. 1979. "Wind generated natural ventilation of housing for thermal comfort in hot humid climates." Fifth International Wind Engineering Conference Proceedings. Pergamon Press.

Aynsley, R.M. 1982. "Natural ventilation model studies." International Workshop on Wind Tunnel Modeling Criteria and Techniques for Civil Engineering Applications Preprints, Timothy A. Reinhold, ed., April 14-16, 1982, pp. V.1-1 - V.1-22.

Aynsley, R.M. 1985. "Modeling parameters for boundary layer wind tunnel studies of natural ventilation." ASHRAE Transactions, Vol. 91, Part 2A.

Bauman, F.; Ernest, D.; and Arens, E. 1988. ASEAN natural ventilation study: Wind pressure distributions on long building rows in urban surroundings. Center For Environmental Design Research, University of California, Berkeley, CA.

Bookhash, F.M. 1981. "Windtower houses of Bastakeya in Dubai." AS/ISES International Conference on Passive and Hybrid Cooling Proceedings, Miami Beach, Florida, pp. 75-79.

Cermak, J.E.; Peterka, J.A.; Ayad, S.S.; and Poreh, M. 1981. Passive and hybrid cooling developments: Natural ventilation - A wind tunnel study. Fluid Dynamics and Diffusion Laboratory, DOE Contract No. DE-AC03-80CS11510, Colorado State University, Fort Collins, Co.

Chandra, S. 1983. "A design procedure to size windows for naturally ventilated rooms." ASES Passive Solar Conference Proceedings. Glorieta, New Mexico, September 1983.

Clarke, J.A. 1986. Energy simulation in building design. U.K.: Adam Hilger Ltd.

Cook, N.J.. 1973. "On simulating the lower third of the urban adiabatic boundary layer in a wind tunnel." Atmospheric Environment, Vol. 7, 691-705.

Cook, N.J. 1978. "Determination of the model scale factor in wind tunnel simulations of the adiabatic atmospheric boundary layer." Journal of Industrial Aerodynamics, Vol. 2, pp. 311-321.

Cook, N.J. 1982. "Simulation techniques for short test-section wind tunnels: Roughness, barrier and mixing-device methods." International Workshop on Wind Tunnel Modeling Criteria and Techniques for Civil Engineering Applications Preprints, Timothy A. Reinhold, ed., April 14-16, 1982, pp. II.3-1 - II.3-12.

Engineering Sciences Data Unit. 1974, 1975 and 1985. Characteristics of atmospheric turbulence near the ground. Item Nos. 74030, 75001, and 85020, ESDU, London.

Engineering Sciences Data Unit. 1982. Strong winds in the atmospheric boundary layer. Item No. 82026, ESDU, London.

Engineering Sciences Data Unit. 1984. Longitudinal turbulence intensities over terrain with roughness changes for flat or hilly sites. Item No. 84030, ESDU, London.

Fairey, P.W., and Bettencourt, W. 1981. "'La Sucka' - A wind driven ventilation augmentation and control device." AS/ISES International Conference on Passive and Hybrid Cooling Proceedings, Miami Beach, Florida, pp. 196-200.

Holmes, J.D. 1983. Wind loads on low rise buildings - A review. Commonwealth Scientific and Industrial Research Organization, Division of Building Research, Victoria, Australia.

Hussain, M., and Lee, B.E. 1980. "A wind tunnel study of the mean pressure forces acting on large groups of low-rise buildings." Journal of Wind Engineering and Industrial Aerodynamics, Vol. 6, pp. 207-225.

Lee, B.E.; Hussain, M.; and Soliman, B.F. 1979. A method for the assessment of the wind induced natural ventilation forces acting on low rise building arrays. Department of Building Science, University of Sheffield, Report No. BS50.

Mattingly, G.E., and Peters, E.F. 1977. "Wind and trees: Air infiltration effects on energy in houses." Journal of Industrial Aerodynamics, Vol. 2, No. 1.

Mattingly, G.E.; Harrje, D.T.; and Heisler, G.M. 1979. "The effectiveness of an evergreen windbreak for reducing residential energy consumption." ASHRAE Transactions, Vol 85, Part 2.

Peterka, J., and Cermak, J. 1975. "Turbulence in building wakes." Proceedings: 4th International Conference on Wind Effects on Building and Structures, London, September 1975, Cambridge University Press.

Peterka, J.A.; Zambrano, T.G.; and Cermak, J.E. 1979. "Effect of an adjacent building on wind pressures." ASCE Annual Convention and Exposition Proceedings, Atlanta, Georgia.

Sherman, M.H., and Grimsrud, D.T. 1982. "Wind and infiltration interaction for small buildings." Annual Meeting of the American Society of Civil Engineers Proceedings, New Orleans, LA, October 23-29, 1982.

Soliman, B.F. 1973. The effect of building grouping on wind induced natural ventilation. University of Sheffield, Department of Building Science, Report BS 14.

Swami, M.V., and Chandra, S. 1987. Procedure for calculating natural ventilation airflow rates in buildings. ASHRAE, Final Report, FSEC-CR-163-86.

Vickery, B.J. 1981. "The use of the wind tunnel in the analysis of naturally ventilated structures." AS/ISES International Passive/Hybrid Cooling Conference Proceedings, Miami Beach, Nov. 1981, pp. 728-742.

Vickery, B.J.; Baddour, R.E.; and Karakatsanis, C.A. 1983. A study of the external wind pressure distributions and induced internal ventilation flow in low-rise industrial and domestic structures. Boundary Layer Wind Tunnel Laboratory University of Western Ontario, Report No. BLWT-SS2-1983.

Wannenburg, J.J. 1957. "Performance testing of roof ventilators." Heating, Piping & Air Conditioning (ASHAE Journal Section), March 1957, pp. 147-154.

Wiren, B.D. 1985. Effects of surrounding buildings on wind pressure distribution and ventilation heat losses for single-family houses. Part 1: 1 1/2-Storey detached houses. The National Swedish Institute for Building Research, Gävle, Sweden, Report No. M85:19.

Wiren, B.D. 1987. Effects of surrounding buildings on wind pressure distribution and ventilation heat losses for single-family houses. Part 2: 2-Storey terrace houses. The National Swedish Institute for Building Research, Gävle, Sweden, March 1987.

ACKNOWLEDGMENTS

The authors wish to thank Mark Levine and Hashem Akbari of Lawrence Berkeley Laboratory for their financial support and technical assistance with this research. We also wish to acknowledge Davide Garda of the UC Berkeley Architecture Department for his help with preparation of model construction drawings and figures for the final report. The IBM personal computer equipment used for data acquisition and analysis throughout this study was provided through an IBM DACE Grant.

TABLE 1

Tap Locations for Average Pressure Measurements

Surface	Tap Locations Model #1	Model #2
Front Facade	3 + 6	27 + 30
Back Facade	19 + 22	43 + 46
Front Jack Roof	11 + 12	35 + 36
Back Jack Roof	13 + 14	37 + 38
Courtyard	19 + 22 + 27 + 30	

TABLE 2

Correlations For Average Surface Pressure Coefficients*

Correlation Equation: $C_p = C_o + \sum_{i=1}^{N} C_i.F_i$

A) Model Configuration: No Jack Roof and No Parapet (NJ,NP); $S_c = 0.5$; $H_c = 0$

Independent Variables (F_i)	Front Facade C_i	Courtyard C_i	Back Facade C_i
Constant	0.095	0.107	--------
$Cos^2\theta$	-0.519	-0.436	-0.602
$Cos\theta * S$	--------	-0.067	--------
$Cos\theta * Ln(S)$	0.571	--------	--------
R^2 (ADJ)	0.980	0.982	0.990

B) Model Configuration: Jack Roof (J,NP) and (J,P); $S_c = 1$; $H_c = 1$

Independent Variables (F_i)	Front Facade C_i	Front Jack C_i	Back Jack C_i	Courtyard NP C_i	Courtyard P C_i	Back Facade C_i
Constant	0.062	-0.240	--------	0.091	-0.082	--------
$Cos^2\theta$	-0.945	-0.098	-0.832	-0.512	-0.512	-0.690
$Cos\theta * S$	0.237	--------	--------	-0.057	-0.057	--------
$Cos\theta * Ln(S)$	--------	0.095	--------	--------	--------	--------
$Cos^2(\theta-45°)$	--------	0.539	--------	--------	--------	--------
R^2 (ADJ)	0.954	0.843	0.985	0.958	0.986	0.993

* Notes

1) Roof slope is $\alpha = 20°$.
2) Refer to Table 1 for definitions of surface tap locations.
3) Correlations for Front Facade and Front Jack, are reported for Model #1 only.
4) Correlations for Back Jack are reported for Models #1 and #2.
5) Correlations for Back Facade are reported for Model #2 only.
6) Ranges of applicability for these correlations are:
   $0 \leq \theta \leq 90°$
   $1 \leq S \leq 5$

TABLE 3

Correlation For Average Surface Pressure Coefficients : Courtyard Effects*

Correlation Equation: $C_p = C_o + \sum_{i=1}^{N} C_i.F_i$

Model Configuration: Jack Roof and Parapets (J,P); S = 1

Independent Variables (F_i)	Courtyard C_i
Constant	--------
$Cos^2\theta$	-0.471
$H_c * S_c$	-0.147
R^2 (ADJ)	0.989

* Notes

1) Roof slope is $\alpha = 20°$.
2) Refer to Table 1 for definitions of surface tap locations.
3) Ranges of applicability for this correlation are:
   $0 \leq \theta \leq 90°$
   $0.25 \leq S_c \leq 1$
   $0 \leq H_c \leq 1$

TABLE 4

Key to Figures and Correlations

#1 - Model # 1 or Windward Model
#2 - Model # 2 or Leeward Model
P - with Parapets
NP - without Parapets
J - with Jack Roof
NJ - without Jack Roof

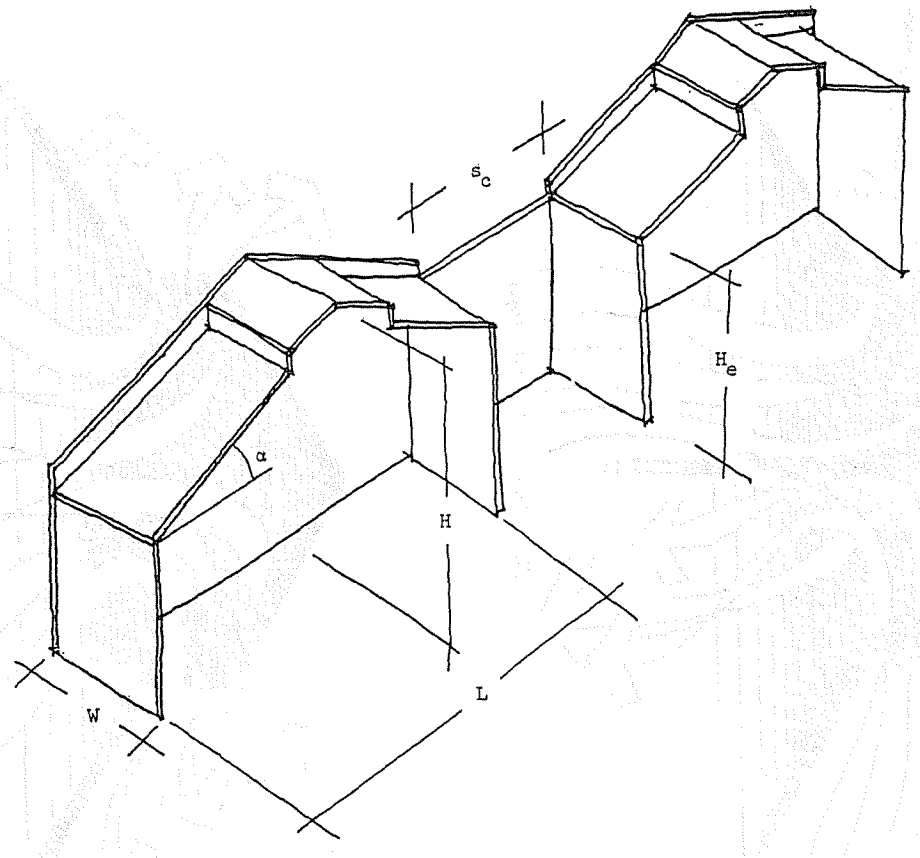

Figure 1a Shophouse test model

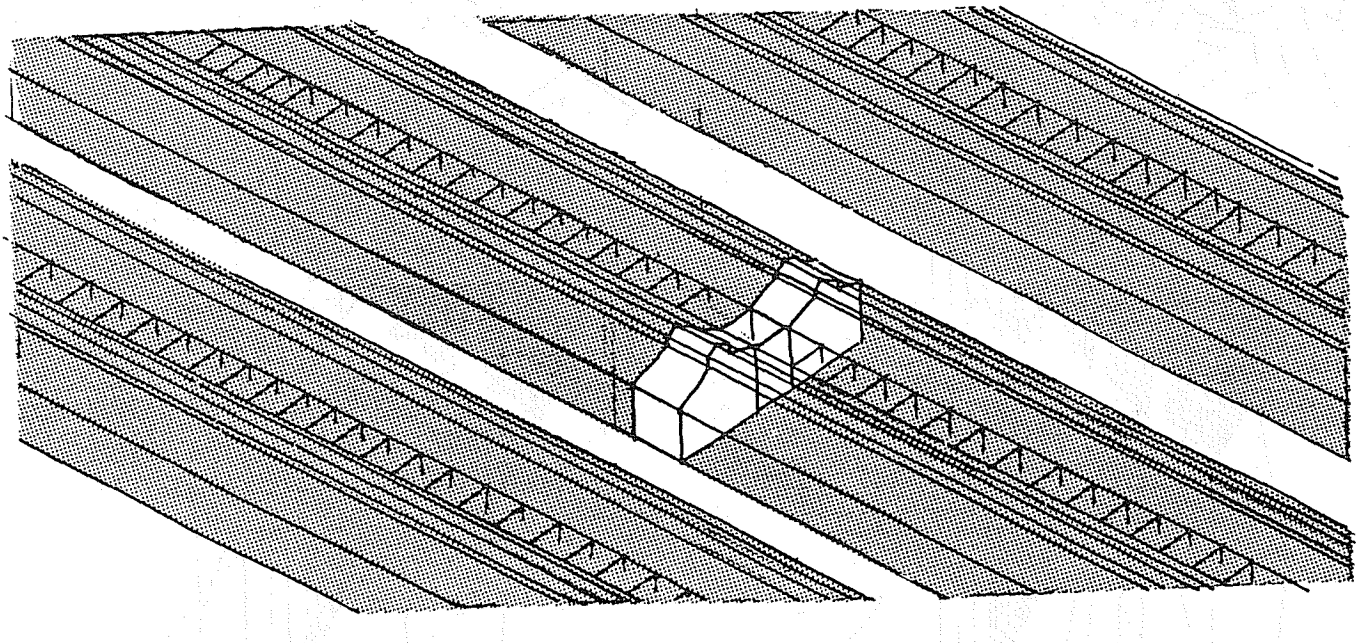

Figure 1b Test unit in row

Figure 2 Jack roof flow configurations

Figure 3 Boundary layer wind tunnel configuration

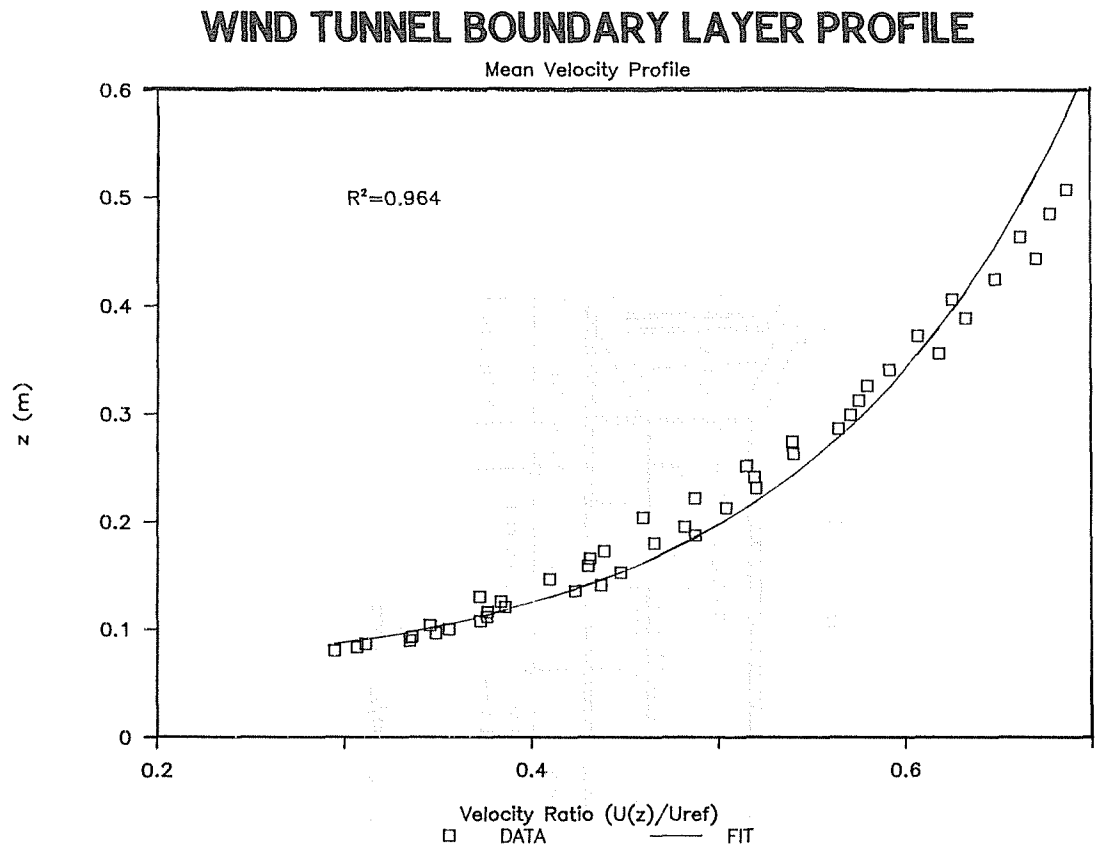

Figure 4a Wind tunnel boundary layer profile: mean velocity profile

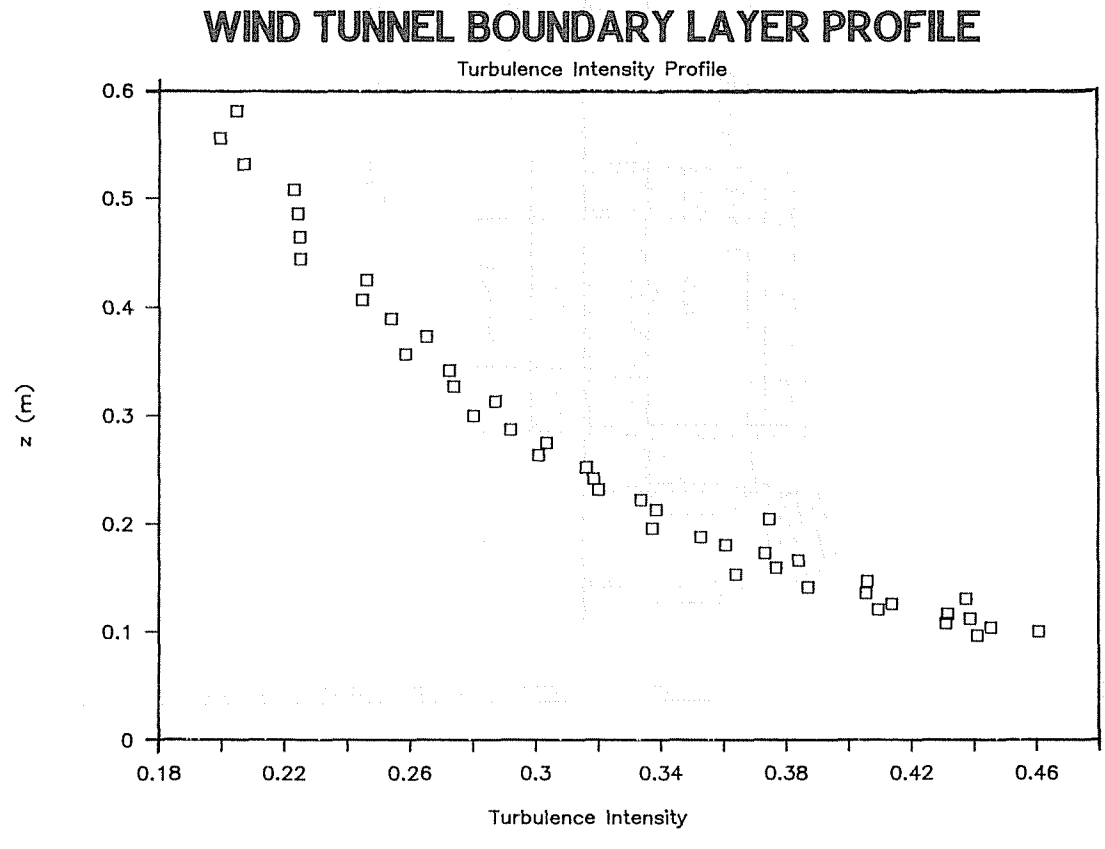

Figure 4b Wind tunnel boundary layer profile: turbulence intensity profile

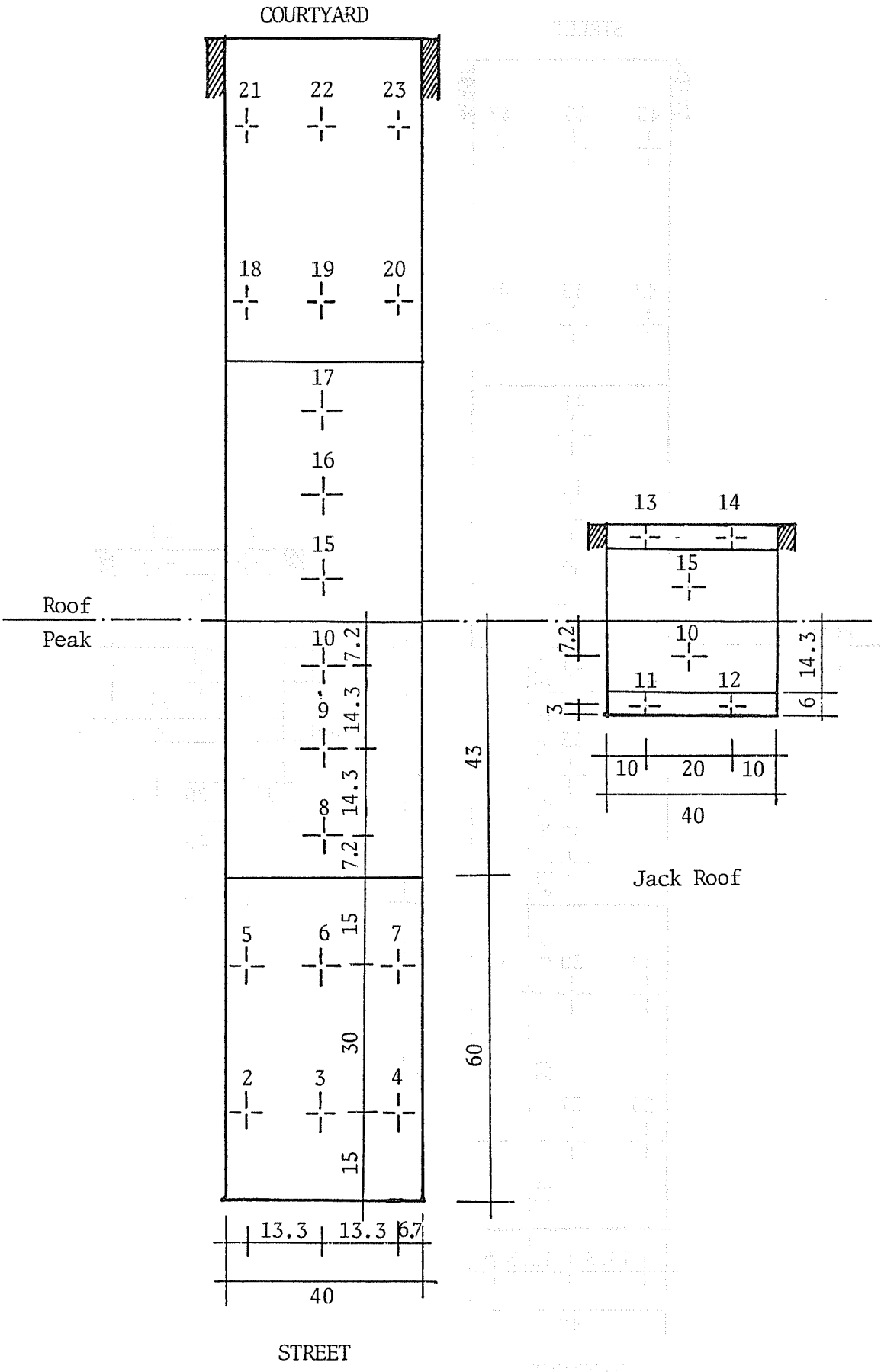

Figure 5a Tap locations for model #1 (dimensions in mm)

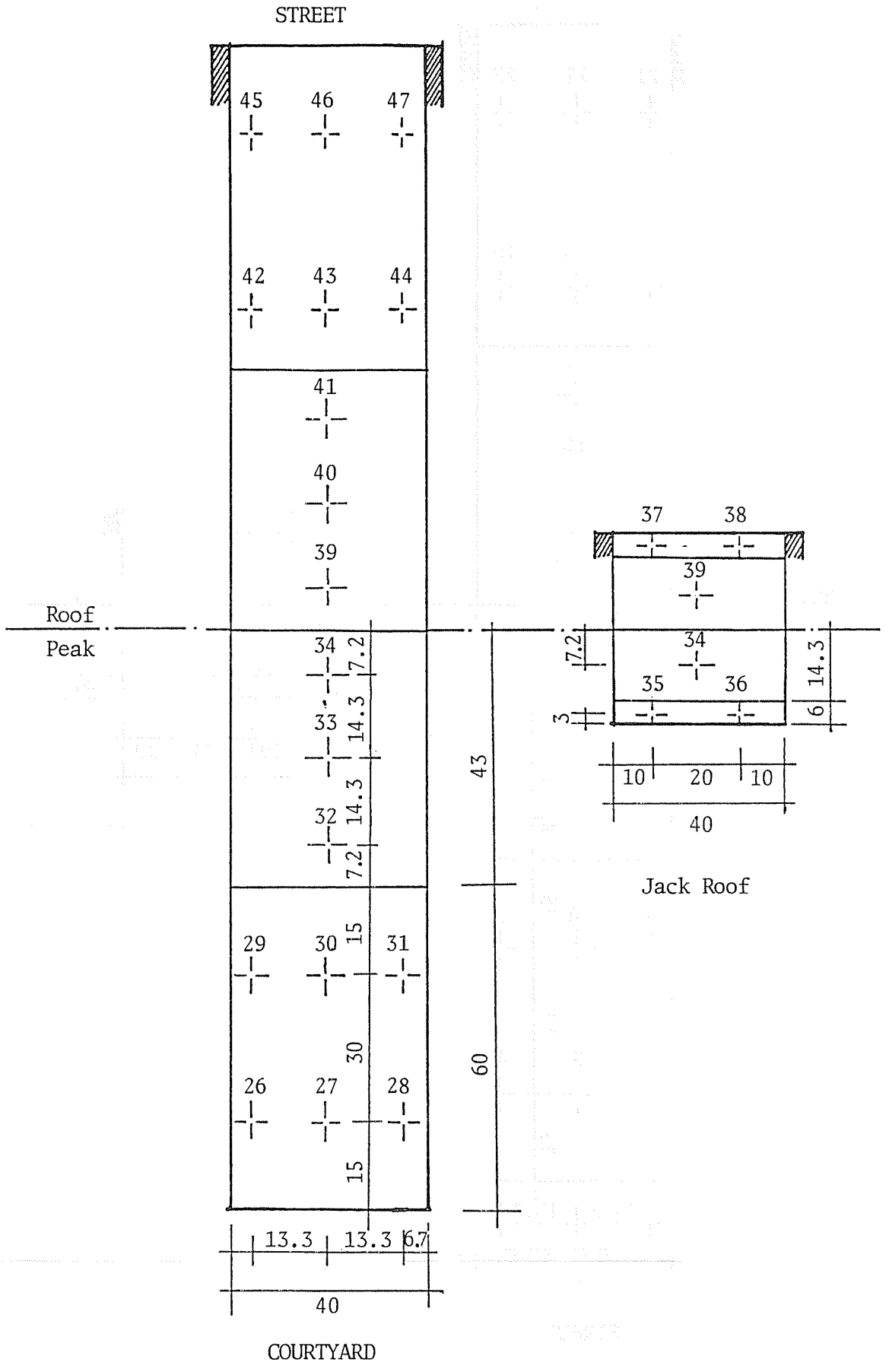

Figure 5b Tap locations for model #2 (dimensions in mm)

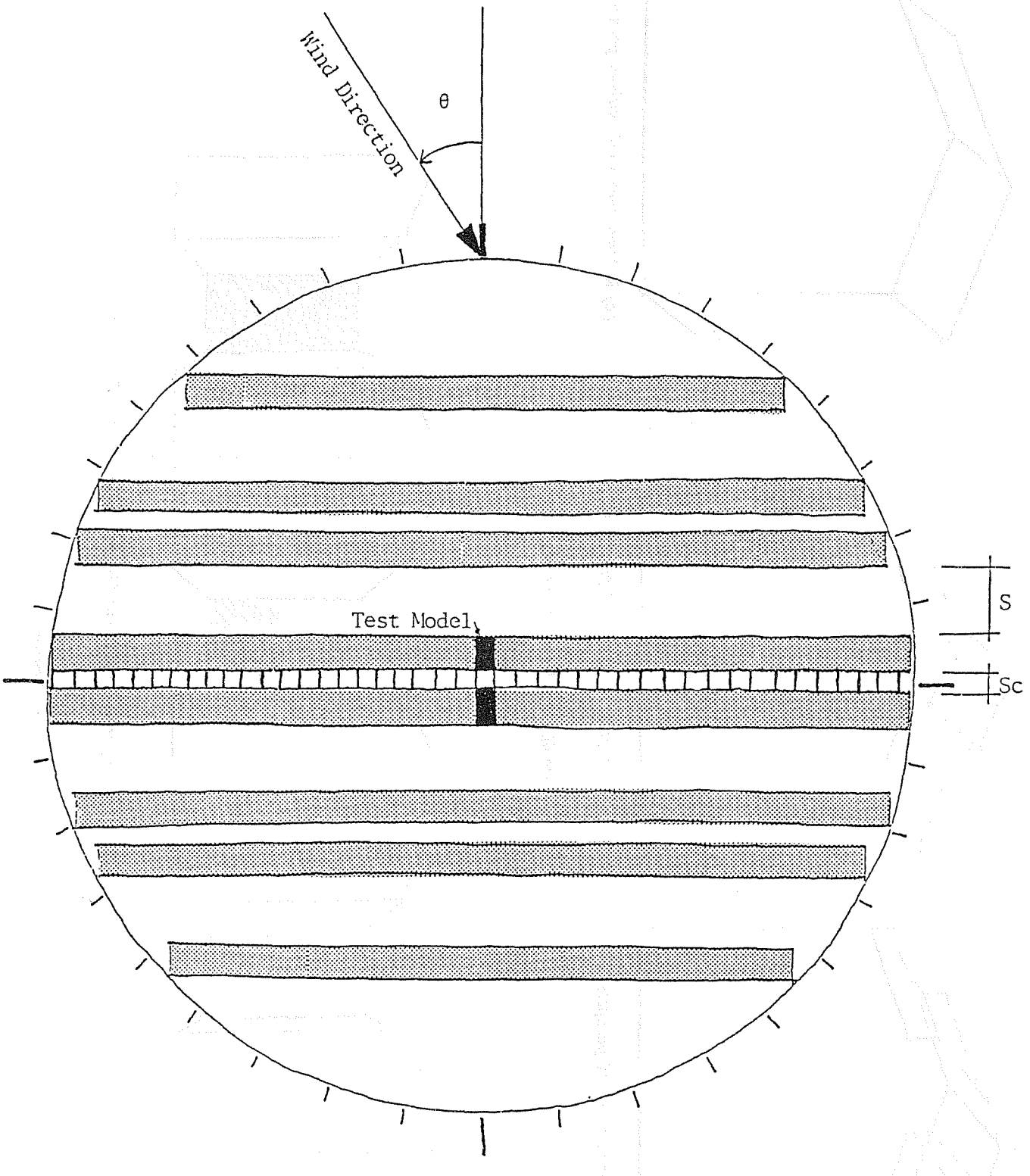

Figure 6a Model spacing configuration and wind direction

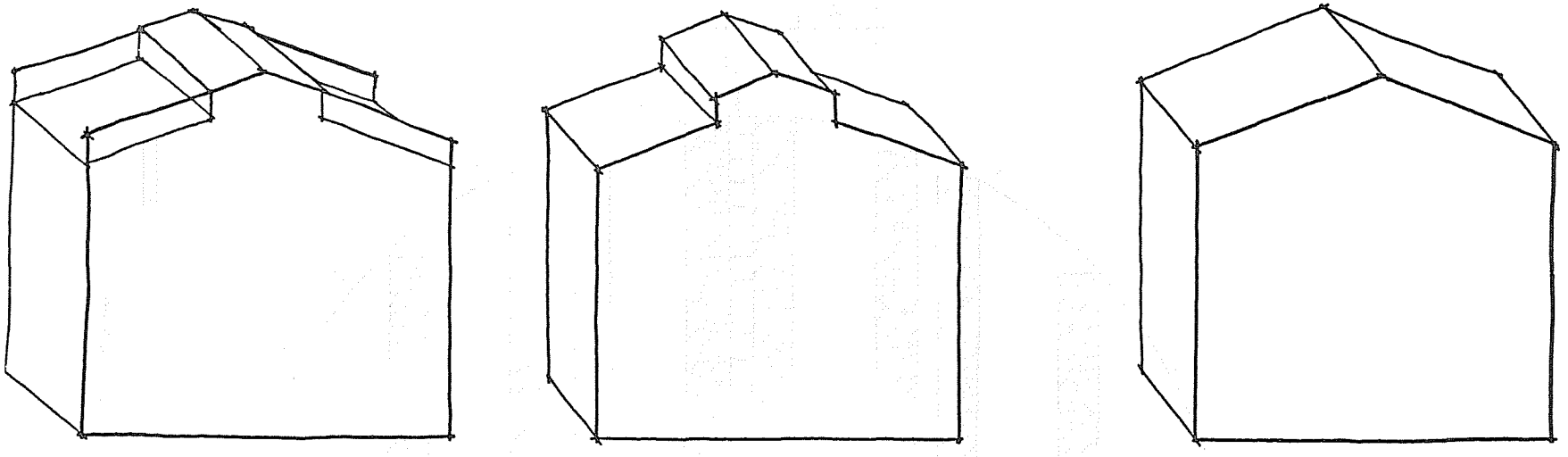

(a) With jack roof and parapets *(b) With jack roof, without parapets* *(c) Without jack roof, without parapets*

Figure 6b Roof configurations

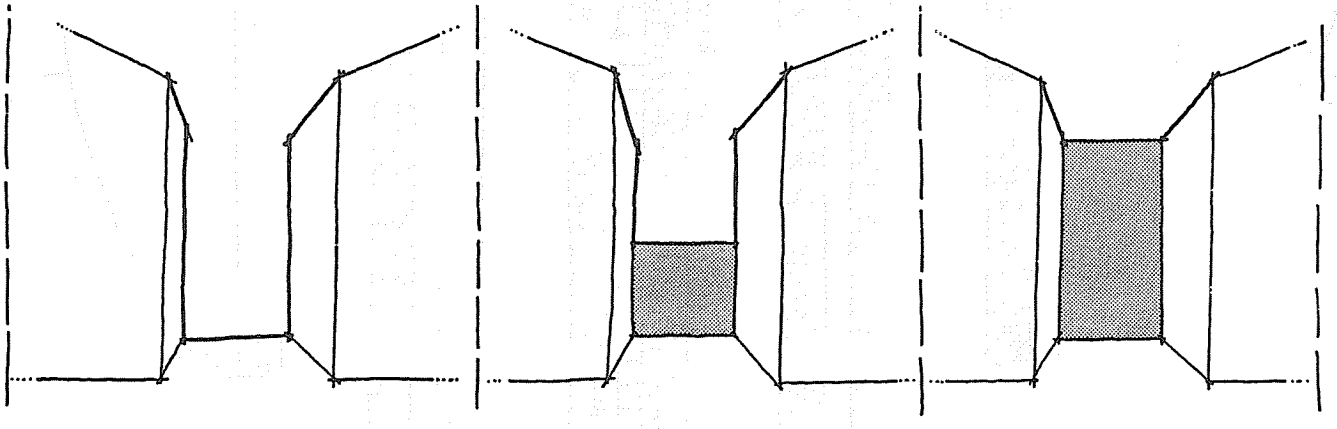

(a) No wall ($H_c = 0$) *(b) Half height wall ($H_c = 0.5$)* *(c) Full height wall ($H_c = 1$)*

Figure 6c Courtyard configurations

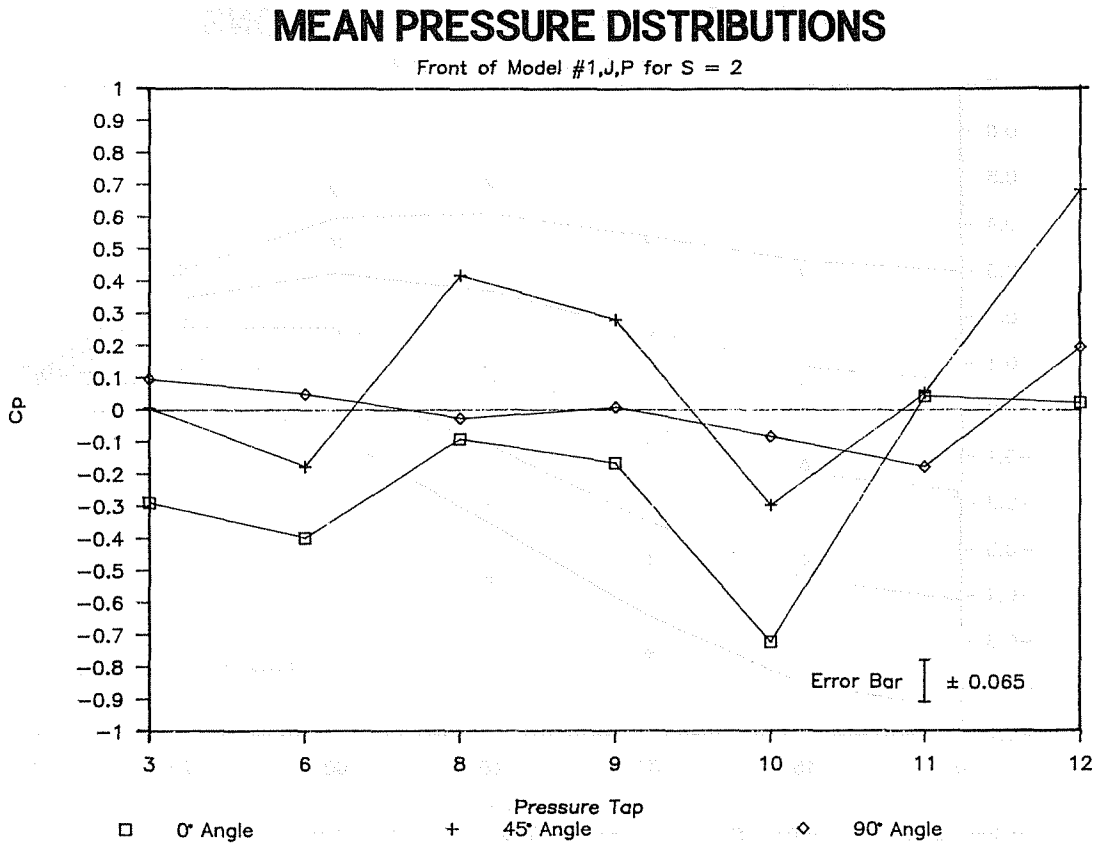

Figure 7a Mean pressure distributions: Front of model #1, J, P for S = 2

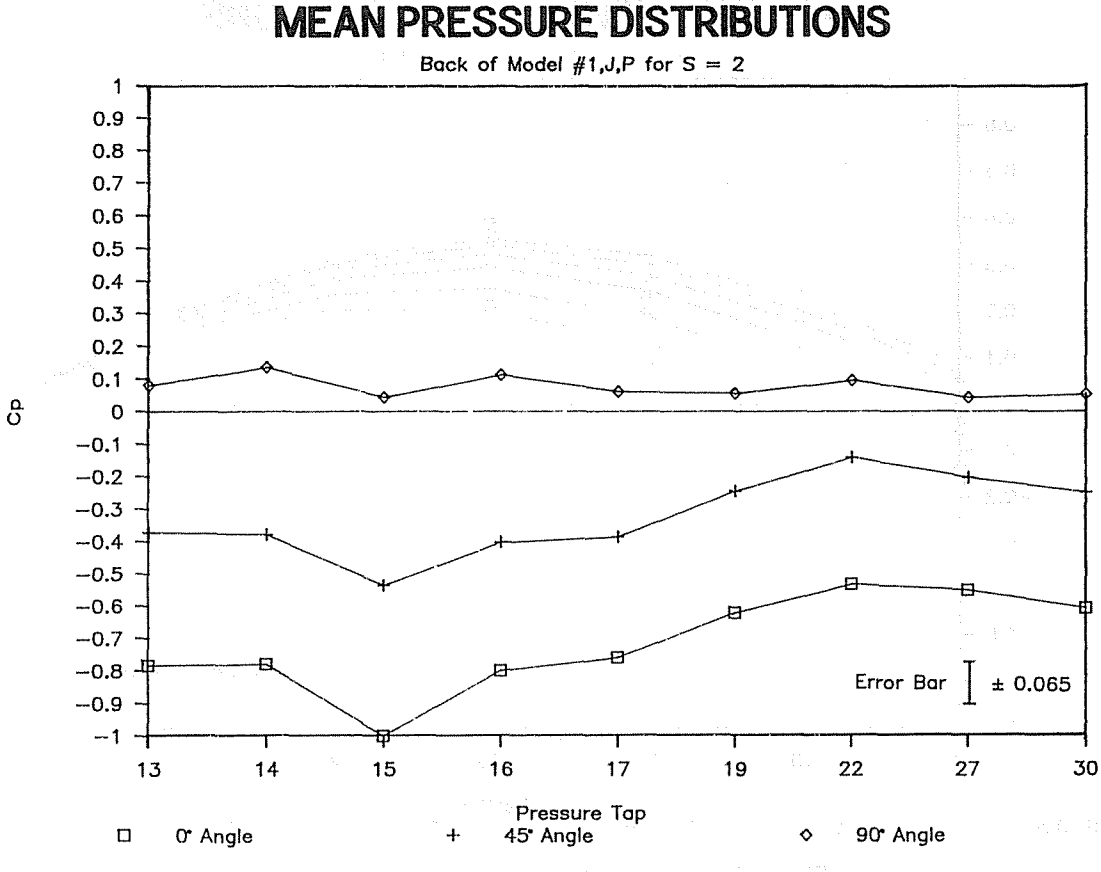

Figure 7b Mean pressure distributions: Back of model #1, J, P for S = 2

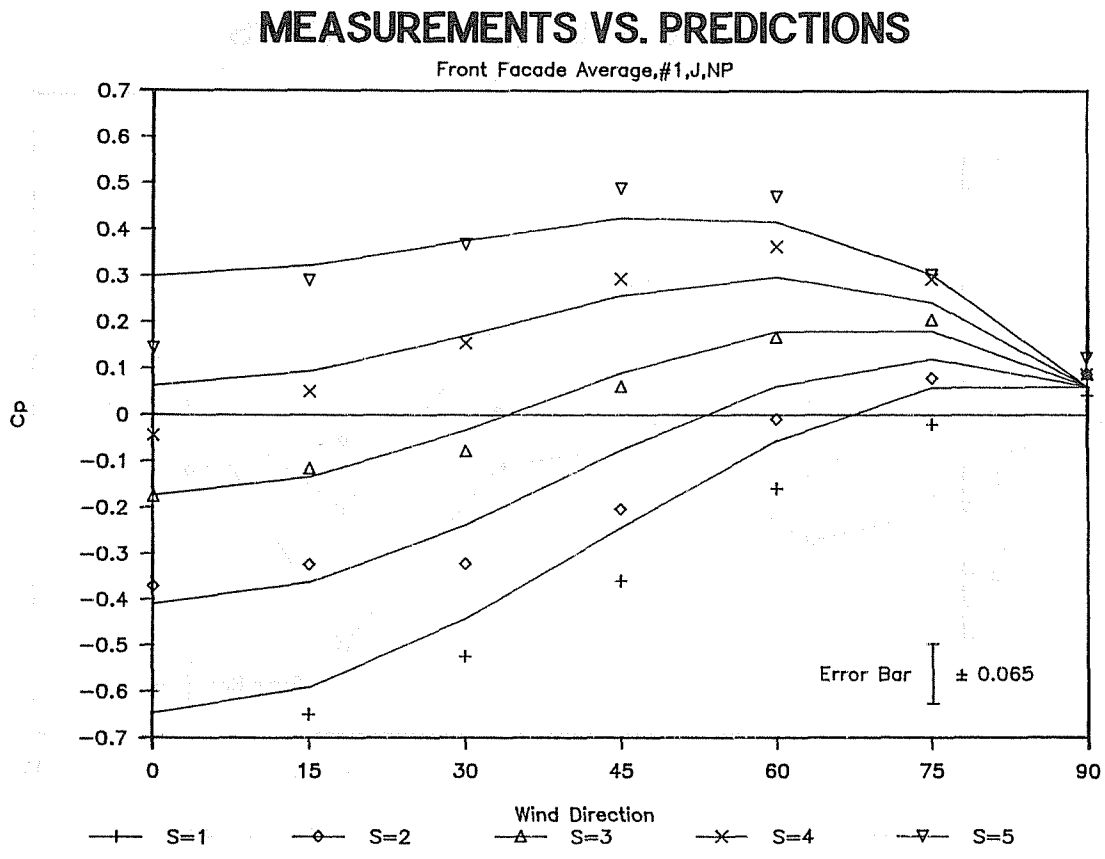

Figure 8a Measurements vs predictions: Front facade average, #1, J, NP

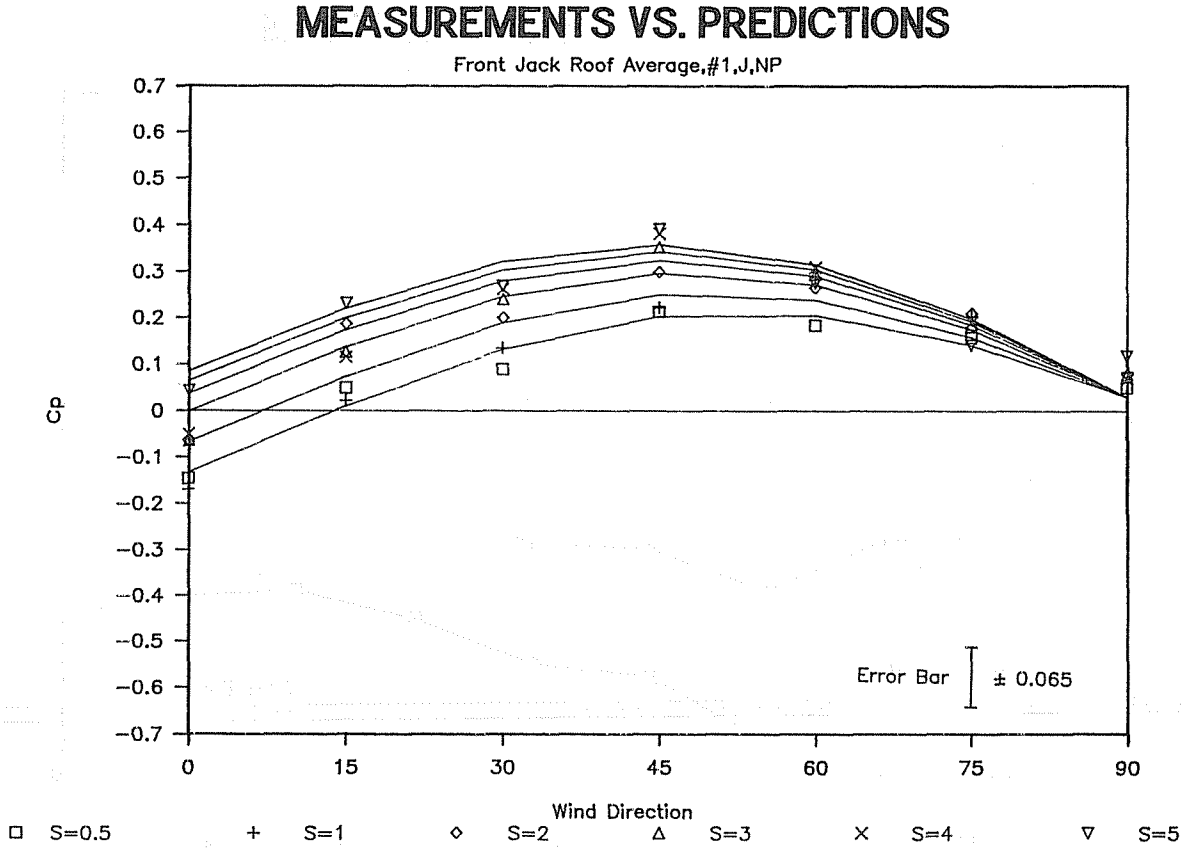

Figure 8b Measurements vs predictions: Front jack roof average, #1, J, NP

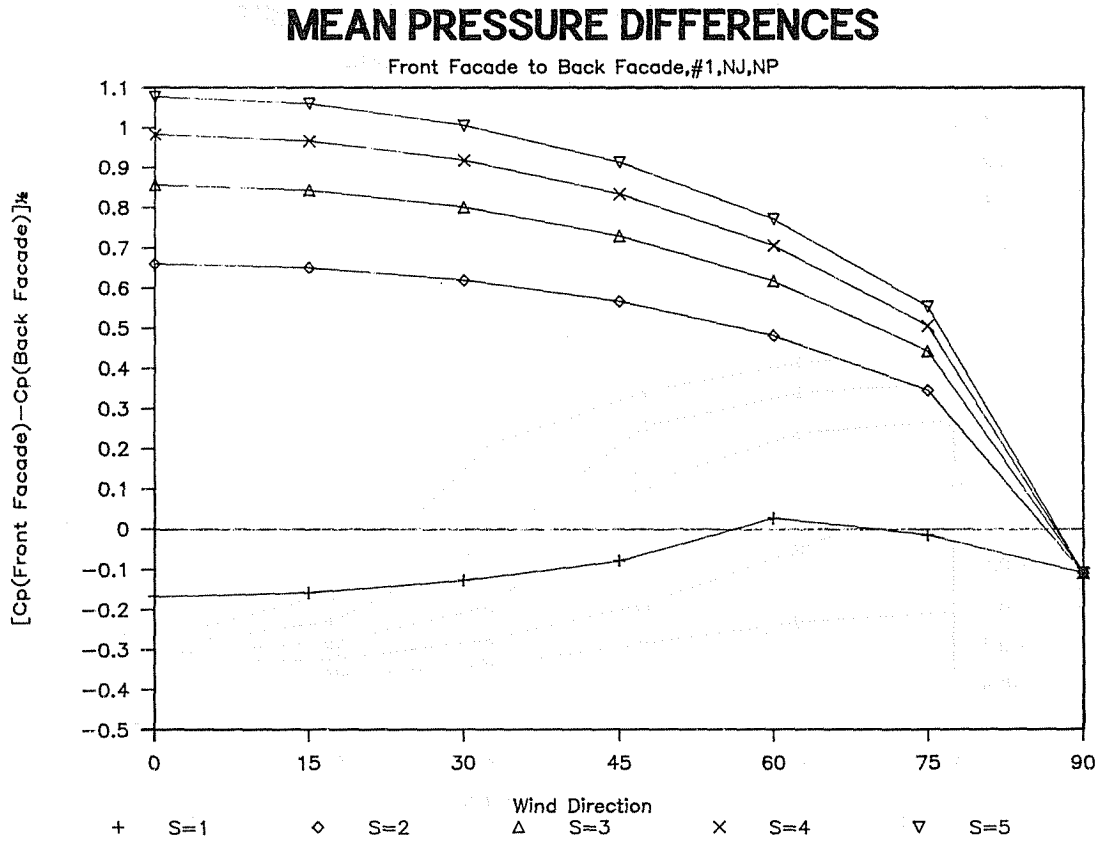

Figure 9 Mean pressure differences: Front facade to back facade, #1, NJ, NP

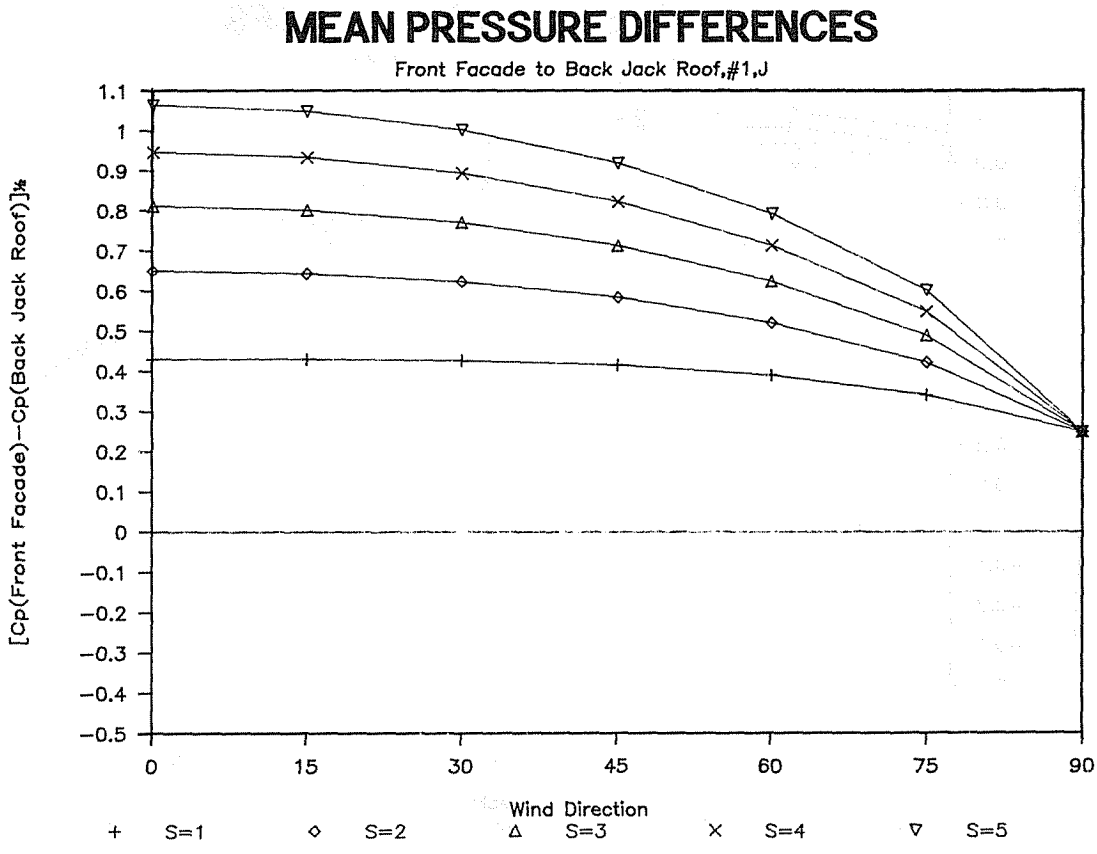

Figure 10a Mean pressure differences: Front facade to back jack roof, #1, J

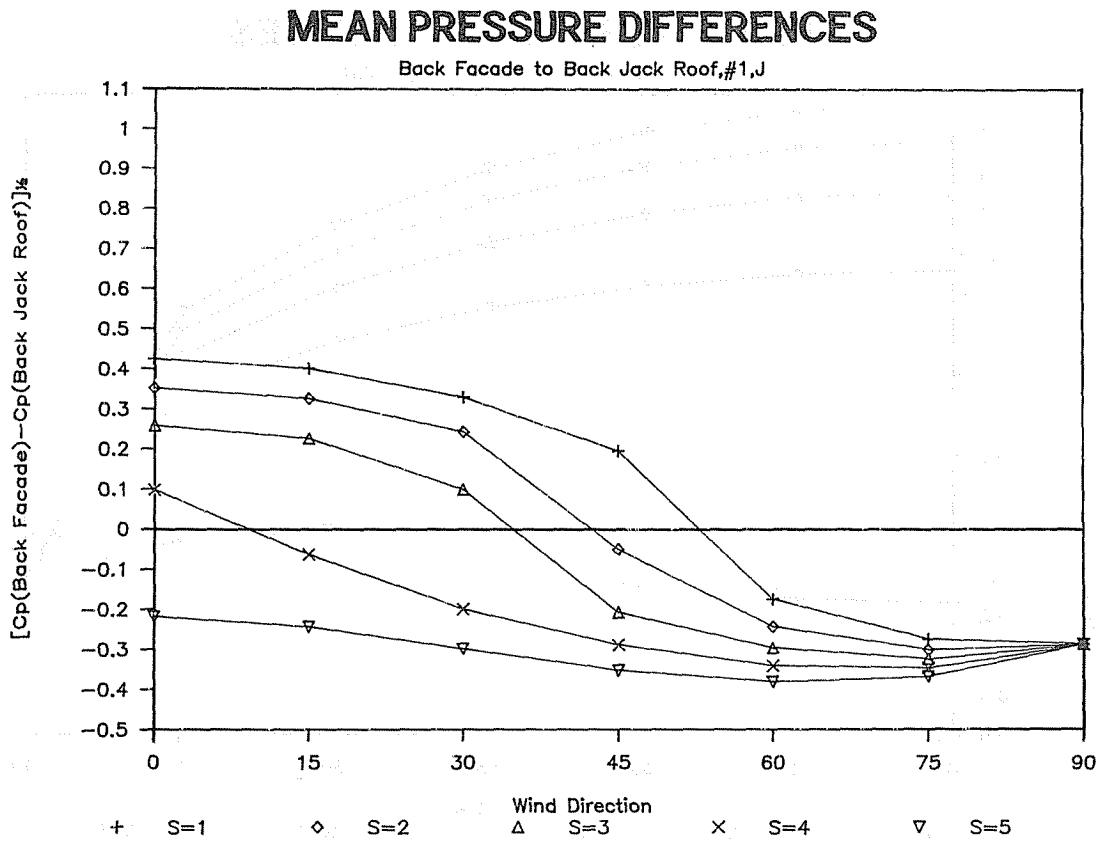

Figure 10b Mean pressure differences: Back facade to back jack roof, #1, J

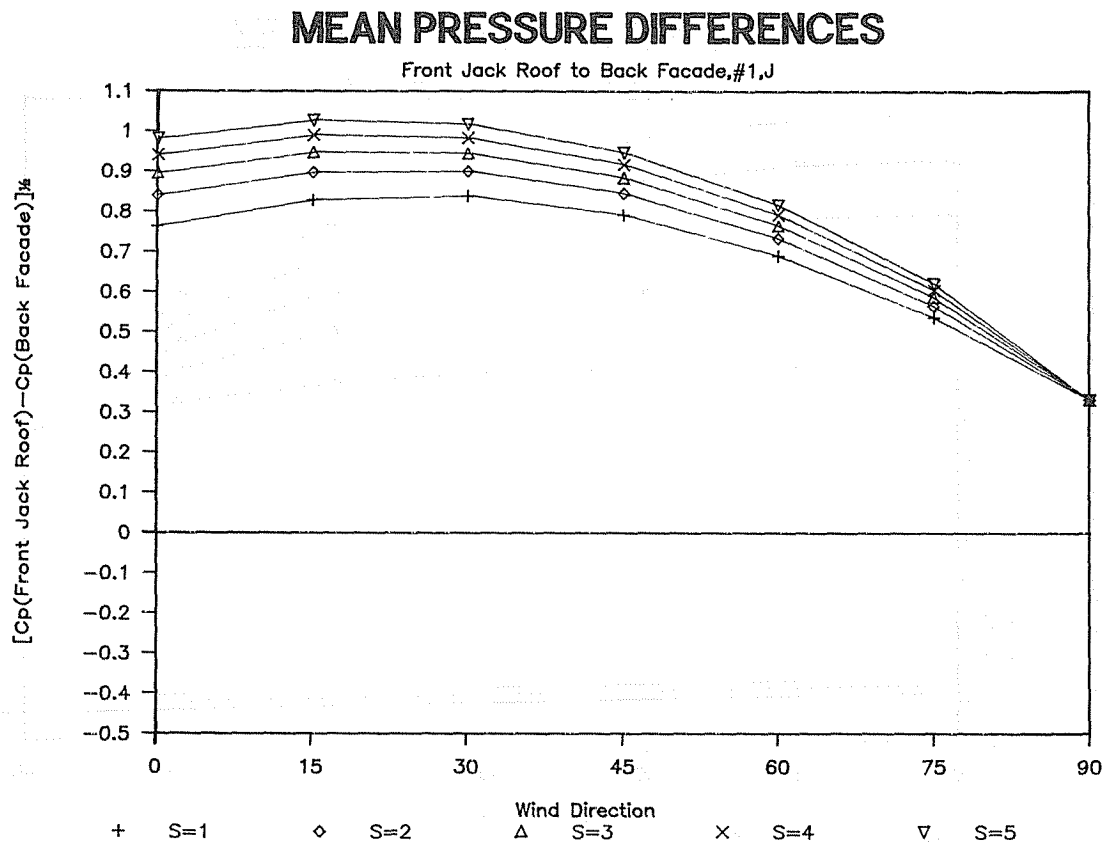

Figure 11a Mean pressure differences: Front jack roof to back facade, #1, J

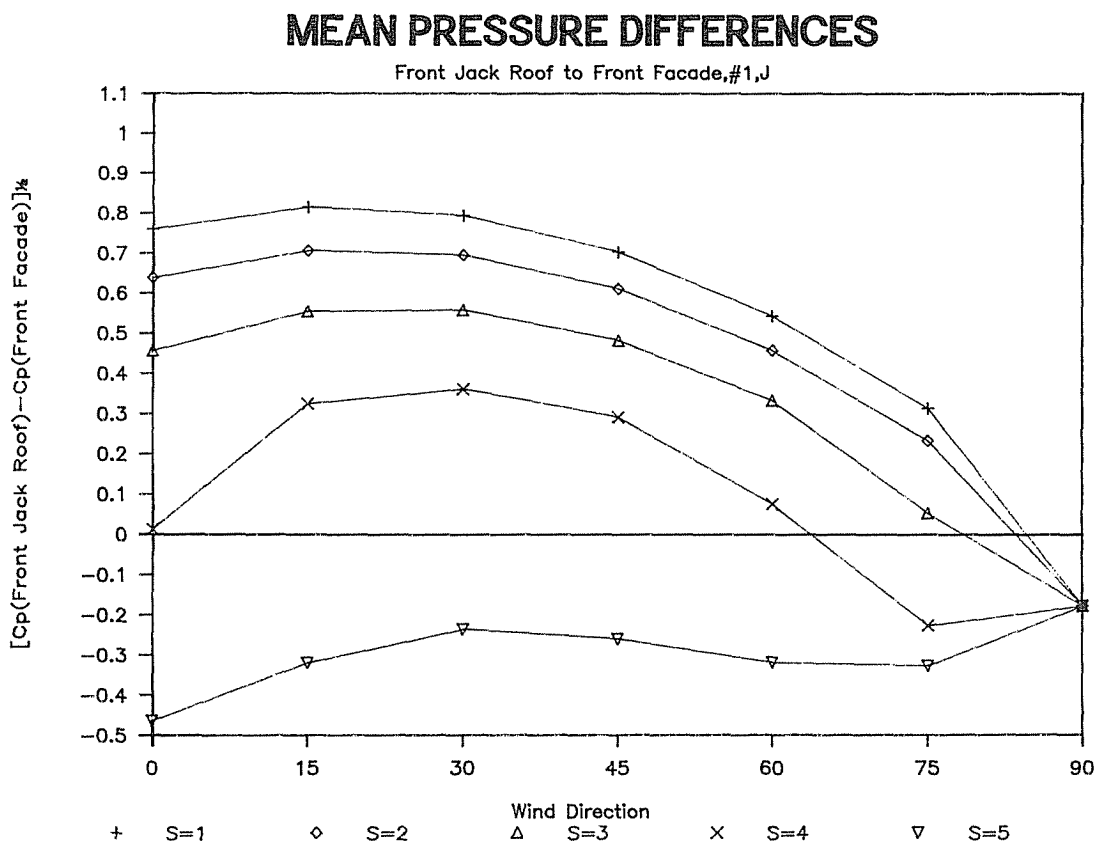

Figure 11b Mean pressure differences: Front jack roof to front facade, #1, J

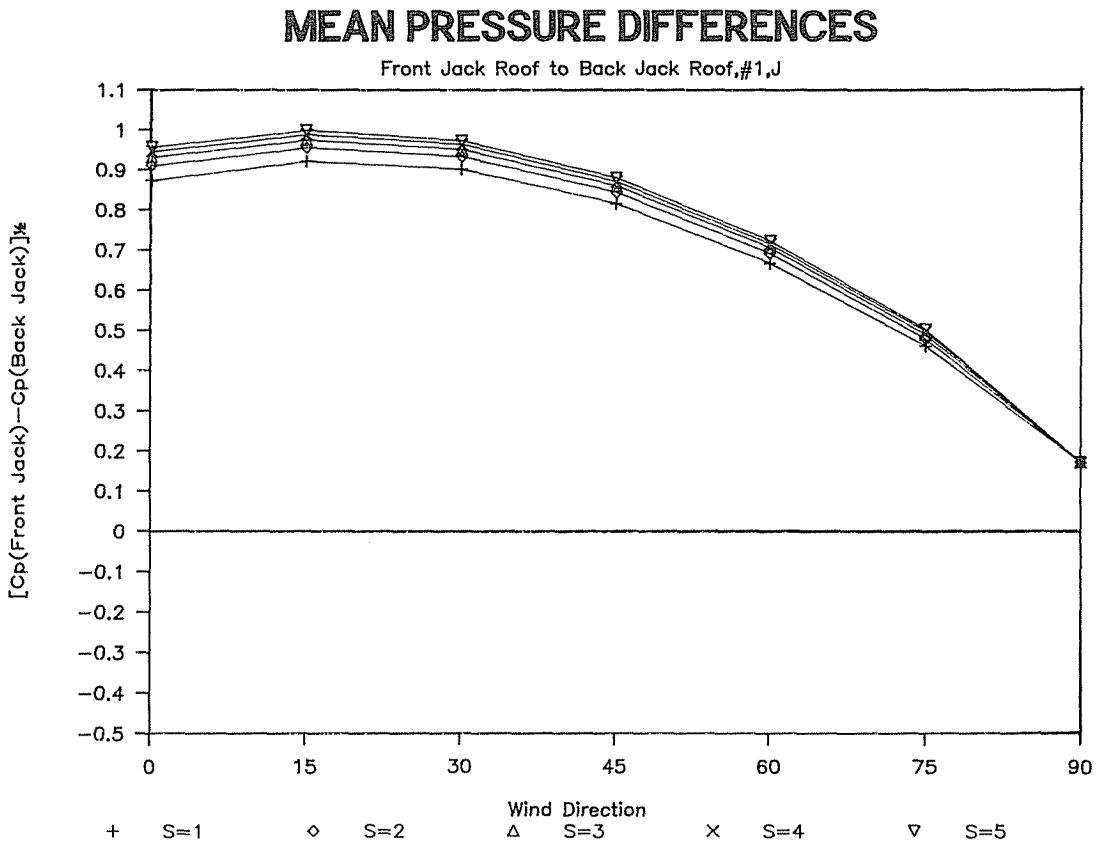

Figure 12 Mean pressure differences: Front jack roof to back jack roof, #1, J